Charge-state dependence of M-shell x-ray production in $_{67}$Ho by 2–12-MeV carbon ions

Y. C. Yu and H. L. Sun
Academia Sinica, Institute of Physics, Nanking, Taipei, Taiwan 11529

J. L. Duggan, F. D. McDaniel, and J. Y. Yin
Ion Beam Modification and Analysis Laboratory, Department of Physics, University of North Texas, Denton, Texas 76203

G. Lapicki
Department of Physics, East Carolina University, Greenville, North Carolina 27858
(Received 16 November 1994)

Charge-state dependence of M-shell x-ray production cross sections of $_{67}$Ho bombarded by 2–12-MeV carbon ions, with and without K-shell vacancies, were measured using a windowless Si(Li) x-ray detector with a full-width-at-half-maximum resolution of 135 eV at 5.9 keV. Carbon ions of different charge states were produced using a postacceleration, nitrogen gas stripping cell. The carbon ions were then magnetically analyzed to select the desired charge state and energy before entering the target chamber. The total M-shell and $M\zeta$, $M\alpha,\beta$, and $M\gamma$ x-ray cross sections were measured. The electron-capture (EC) contributions as well as the direct-ionization (DI) contributions can be determined by making a comprehensive study of the projectile-charge-state dependence of the target x-ray production cross sections for targets in which the single-collision realm is maintained. In this paper, both EC and DI contributions and the total M-shell x-ray production cross sections are compared to both the first Born theory and to the perturbed-stationary-state theory with energy-loss, Coulomb-deflection, and relativistic corrections.

PACS number(s): 34.70.+e, 34.50.Fa

I. INTRODUCTION

Direct ionization (DI) and electron capture (EC) lead to inner-shell ionization in ion-atom collisions. It is known that DI is the dominant mechanism if $Z_1/Z_2 \ll 1$ and $v_1/v_{2S} \gg 1$, where Z_1 and Z_2 are the atomic numbers of the projectile and target atom and v_1 and v_{2S} are the projectile velocity and the target inner-shell ($S=K$, L, and M shell, etc.) electron velocity, respectively. However, for larger ratios of Z_1/Z_2 and smaller ratios of v_1/v_{2S}, EC plays an increasingly important role. Most of the measurements for K-, L-, and M-inner-shell ionization are compared to the DI calculations. The EC role can be determined by making a comprehensive study of the projectile charge-state dependence of the target x-ray production cross section for targets in which the single collision realm is maintained. The single collision regime is determined through the study of the effective cross sections for target x-ray production for various charge states as a function of target thicknesses. These studies are critical to the theoretical analysis since the electron configuration of the projectile in a solid target is not very well understood, as was described in a review article by Betz [1].

Charge-state considerations in atomic physics problems have been in evidence for nearly half of a century, starting with the classic works of Bohr [2] and Allison and Warshaw [3], who analyzed charge changing collisions through stopping power measurements. The first reported work on charge-state effects in x-ray yields for ion-atom collisions was made in 1972 by Macdonald *et al.* [4]. They showed that for 35.7-MeV fluorine ions, the x-ray yield in argon, krypton, and xenon was dependent on the incident charge state with the yields increasing as much as a factor of 5 for the higher charge states. This paper was followed by another from the same group [5], as well as from Mowat *et al.* [6] and Brandt *et al.* [7]. The first theoretical paper to address these data was by Halpern and Law [8] in which they showed that the high Z dependence of the x-ray yield could be accounted for by including K-shell charge exchange into bound states of the fully stripped projectile. These early calculations stimulated other measurements in 1974 and 1975 by Macdonald and co-workers [9] and also by Hopkins *et al.* [10]. In 1976, Macdonald *et al.* [11] studied the dependence of K-shell x-ray production in nearly symmetric collisions for highly ionized S and Cl ions in gases. Their EC data as well as data that were reported subsequently in Refs. [12–21] were analyzed using different scaling numbers to adjust the cross sections calculated in the Oppenheimer-Brinkman-Kramers approximation [22] to these data. Most of their papers dealt with K-shell x-ray measurements, charge state and target thickness dependence to establish the single collision regime.

In 1977, McDaniel *et al.* [23] studied the projectile charge-state dependence of target K-shell ionization by 1.86-MeV/u Si ions. Their data provided supporting evidence for the precursor for the perturbed-stationary-state theory with energy-loss, Coulomb-deflection, and relativistic corrections (ECPSSR) of electron capture with reduced binding. Adopting calculations of Lapicki and Losonsky [24], McDaniel *et al.* [23] demonstrated that no such empirical scaling factors were required to analyze the projectile–charge-state dependence in K-shell ionization by silicon ions. In 1979, McDaniel *et al.* [25] extended the projectile charge-state dependence studies to target L-shell ionization by 1.86-MeV/u fluorine and silicon ions and 1.8-MeV/u chlorine ions. The present authors and others have measured and analyzed K-,

L-, and M-shell ionization data in a variety of collision systems [26–44].

To date, no data have been reported in the study of EC contribution to M-shell ionization below 1 MeV/u. The major experimental problems stem from the fact that the energies of M-shell x rays are less than about 3 keV. For the rare-earth region, M-shell binding energies and x-ray energies are of the order of 1 keV. Conventional Si(Li) x-ray detectors have an 8.5-μm beryllium window that is opaque to these soft x rays and hence, the lack of data in the literature. We have been able to resolve this experimental problem by installing a windowless Si(Li) x-ray detector and a UHV chamber on one of the beam lines of the 3-MV tandem accelerator. With this system, x-ray energies down to 282 eV ($_6CK\alpha$) have been measured [36,39]. We have recently reported M-shell x-ray production cross sections for eleven rare-earth elements from $_{72}$Hf to $_{57}$La by 0.6–4.6-MeV protons [43] and 0.7–7.0-MeV alpha particles [44]. During the course of these experiments, considerable experience has been developed in producing thin and contaminant-free rare-earth targets and in measuring the 0.64–1.9-keV x rays that result from M-shell ionization.

To study both DI and EC contributions to M-shell ionization, $^{12}_6C^{q+}$ ions in the energy range from 2–12 MeV were used to bombard $_{67}$Ho targets. A $_{67}$Ho target of 0.34 μg/cm^2, which is thin enough to be in the single collision regime, was used for the present studies. The target thickness measurements, as a function of charge state to be shown later in this paper, will show that $^{12}C^{5+}$ and $^{12}C^{6+}$ have single collisions in $_{67}$Ho targets which are less than 2 μg/cm^2. The M-shell x-ray production cross sections have been measured for the 0.34-μg/cm^2 $_{67}$Ho target for ^{12}C energies from 2 to 12 MeV and for charge states 2+, 3+, 4+, 5+, and 6+. These data will be compared with predictions of the first Born [45,46] and the ECPSSR theories [24,47–50]. This present set of measurements should provide the first reported study of the EC and DI contributions in the regime of $Z_1/Z_2=0.09$ and $0.17\leq v_1/v_{2M}<0.42$ in M-shell ionization.

II. THEORY

At high ion velocity, where $v_1 \gg v_{2S}$, and for $Z_1 \ll Z_2$, DI is the predominant mechanism [51]. In the DI process, the Coulomb interaction between the ion and target electron promotes a target inner-shell electron into the continuum. At lower ion velocity, $v_1 \leq v_{2S}$, and $Z_1 \leq Z_2$, EC may become important [24]. In the EC process the ion captures an inner-shell electron from the target atom into a vacant bound state of the incident ion. For slow symmetrical ion-atom collisions where $v_1 \ll v_{2S}$ and $Z_1 \approx Z_2$, the dominant vacancy production process involves the formation of a molecular orbital [52–57].

The first Born theory includes two parts, the plane-wave Born approximation (PWBA) [45] for DI and the Oppenheimer-Brinkman-Kramers (OBK) theory modified by Nikolaev [22,46] for EC. The PWBA is a quantum-mechanical method to describe the incident projectile as a plane wave. This theory was first proposed by Bethe [58] for a description of the excitation and ionization processes and then extended by Merzbacher and Lewis [51] to develop a complete picture. The DI process is successfully described by the PWBA for high-velocity projectiles; however, for low-velocity projectiles, the inner-shell electrons of the target atom might be captured to an unoccupied state of the projectile. The OBK theory [22] uses the first Born approximation to describe the transition of an electron from a hydrogenic target to hydrogenic states of a fully stripped ion. The OBK was modified by Nikolaev [46] who used nonrelativistic screened hydrogenic wave functions for calculating electron capture cross sections and is called the OBKN. The PWBA together with the OBKN in the present work is described as the first Born theory. It is this theory that is used for one of the comparisons with the present data.

The ECPSSR theory for DI was implemented by incorporating certain modifications to the appropriate parameters of the first Born theory. Brandt, Basbas, Lapicki, and others [47–49] have included the perturbed stationary state (PSS) in considering the polarization and binding energy effects and relativistic (R) wave functions for the target electron while the projectile is passing near the atomic electron. These calculations also accounted for the energy loss (E) and the Coulomb deflection (C) of the projectile as it traverses the target. The increase in the binding energy of the target inner-shell electrons due to penetration of the projectile inside the inner-shell during the collision reduces the probability for ionization. The polarization of the inner-shell electron wave function due to the projectile, which keeps the projectile and target electron in contact longer, increases the ionization probability. The deflection of the projectile by the Coulomb field of the target atom increases the distance from projectile to the target electron and therefore reduces the ionization probability. The energy loss of the projectile reduces the ionization probability if the $v_1 \ll v_{2S}$. The relativistic effect of the target electron increases the mass of the electron and reduces the ionization probability. Lapicki and Losonsky [24] and Lapicki and McDaniel [50] went beyond the OBKN formalism using the ECPSSR approach for electron capture. Thus, the ECPSSR theory has been extended to the low velocity range where $Z_1/Z_2<1$, and $v_1/v_{2S}<1$. This theory has been shown to give good agreement for a wide variety of K-, L-, and M-inner-shell ionization measurements [36,39,59,60]. Very little data have been reported on M-shell ionization and hence this theory has yet to be fully tested over a wide range of velocities and atomic numbers.

III. EXPERIMENT

The experiment was done at the Ion Beam Modification and Analysis Laboratory (IBMAL) at the University of North Texas (UNT). The negative ions were generated by the SNICS (Source of Negative Ions by Cesium Sputtering) ion source. These ions were first analyzed for momentum/charge by 30° and 90° magnetic spectrometers and then injected into the tandem accelerator. The energetic projectile ions were accelerated with the NEC (National Electrostatic Corporation) 3 MV Model 9SDH-2 tandem accelerator. At the 3-MV maximum terminal voltage of the UNT tandem accelerator, it is not possible to produce usable quantities of the charge state 5+ and 6+ carbon ions by stripping them in the gas canal inside the accelerator. To produce the higher charge states, the accelerated ions were additionally stripped in a postacceleration gas stripping cell. High-resolution magnetic momentum/charge analysis of the ion beam was then

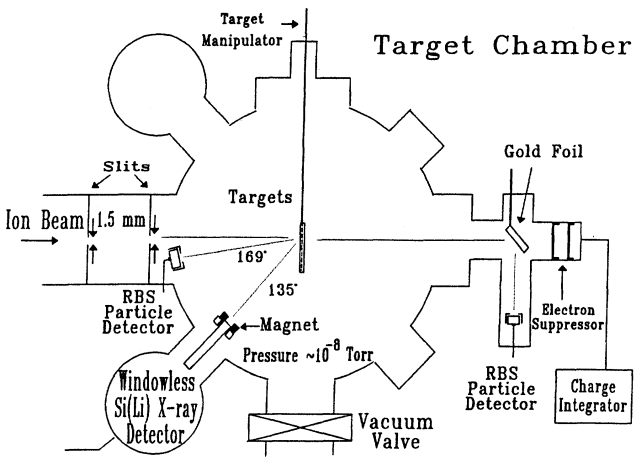

FIG. 1. Schematic diagram of the ultrahigh-vacuum target chamber that was used for the x-ray and scattered particle measurements.

performed at 40° in order to select the desired charge state for transmission into the ultrahigh vacuum ($<10^{-8}$ Torr) beamline.

Figure 1 shows a diagram of the multifunctional target chamber that was used for the x-ray measurements. The beam was collimated by two sets of slits that were 40 cm apart. The first group of slits with a width of 1.5 mm was used for selecting the desired beam and the second group with a width of 0.5–1.5 mm was used to define the beam spot on the target. The target chamber, which was maintained at the pressure below 10^{-8} Torr by a cryopump, has an interlock for target insertion. The target was perpendicular to the beam direction. The targets were made by evaporating the target element onto 5-μg/cm^2 carbon foils. The technique developed by the UNT group for preparing contaminant free targets has been described in Refs. [28,38,61,62]. The Link Analytical windowless Si(Li) x-ray detector was positioned at 135° with respect to the beam direction. A deflecting magnet with a collimator was mounted in front of x-ray detector to eliminate scattered charged particles [63]. The system resolution for this detector for the Mn $K\alpha$ line was 135 eV. An advantage of this detector is, that since it does not have a beryllium window, it can measure x rays down to the boron $K\alpha$ line at 185 eV. In general, Si(Li) detectors have an 8.5-μm beryllium window that precludes measurements below 1 keV. The most difficult problem associated with the Si(Li) detector was in calibrating its efficiency as a function of energy. One normally measures efficiencies by comparing the detector response to standard radioactive sources [64]. These are usually radioisotopes that decay by nuclear electron capture and emit x rays characteristic of the daughter in the decay, which works well for x-ray energies from 3.3 keV up to about 25 keV. The region of interest for our studies was the region around the $_{67}$Ho $M\alpha$ line, which is 1.35 keV. In order to determine the efficiency below the $_{93}$Np $M\alpha$ at 3.3 keV (from $^{241}_{95}$Am decay), two methods were used and these data were then normalized to that obtained from radioactive sources. The first method was to use protons and α particles to bombard low atomic number targets in the investigated x-ray regime [65]. The efficiency of the detector was then determined based on a comparison of the x-ray yields with the ECPSSR theory [47–50]. This theory has been shown to be good to at least 10–20% for these low atomic number K-shell ionization measurements [59]. The second technique of determining the efficiency for this low-energy region relies on the atomic field bremsstrahlung method using 66.5-keV electrons that bombard gold, silver, and aluminum targets. The energy dependence of the bremsstrahlung distribution was measured using the windowless Si(Li) x-ray detector and compared with theory, which gives shape results to $\pm 12\%$ [66]. These bremsstrahlung measurements gave the relative efficiency of the detector, which was then normalized to the proton and α-particle data and radioactive source results. For the present experiment, the region of interest is from the $M\gamma$ (1.58 keV) down to the $M\zeta$ (1.05 keV)for $_{67}$Ho. It is estimated that the absolute efficiency in this region should be valid to at least ± 12–16%. A Rutherford backscattering (RBS) particle detector was mounted at 169° with respect to the beam direction. The solid angle, $\Delta\Omega = \text{area}/R^2 = 6.77\times 10^{-3}$ sr, of the RBS detector was calculated from the area of the defining aperture and the distance R to target. The solid angle was confirmed using a National Institute of Standards and Technology calibrated ^{241}Am source. The x-ray production cross section can be measured, independent of target thickness and beam current fluctuation, by simultaneously measuring x rays and scattered particles for each case. The x-ray production cross section is given by

$$\sigma_X = (Y_X \sigma_R \Delta\Omega t_X)/(Y_R \varepsilon_X S_X t_R), \quad (1)$$

where Y_X and Y_R are the numbers of measured x rays and scattered particles, respectively; σ_R is the theoretical Rutherford differential cross section; t_X and t_R are dead times for the x-ray and backscattered particle measurements, respectively; ε_X is the calibrated intrinsic efficiency plus solid angle of x-ray detector, and S_X is target x-ray attenuation factor [67].

Because the heavy ions traveling through the target may not be in an equilibrium charge state, the charge collected from the Faraday cup after the target chamber cannot be used to determine the number of heavy ions interacting with the target. Some of the present measurements lasted over 10 h in order to get good statistics for the backscattered projectiles. This is because of the $1/E^2$ dependence of the Rutherford cross section and the fact that charge-state dependence measurements can only be done with vanishingly thin targets. In order to reduce the instrumental dead time of the windowless x-ray detector for measuring the high yield of low-energy carbon x rays and bremsstrahlung, the ion beam current was kept below 0.5 nA on the Ho target. To overcome the low counting statistics for the back angle RBS detector (at 169°), a separate postscattering chamber was added (see Fig. 1) after the main scattering chamber. In this postchamber, a 200-μg/cm^2 gold foil was used as a scattering foil, which produces a large backscattered particle yield. A second RBS detector was used to count scattered $^{12}C^{q+}$ ions at 90° with respect to the beam direction in this post chamber. The ratio of the $_{67}$Ho target back angle RBS yield at 169° is always proportional to the gold scattering yield at 90°. The $_{67}$Ho

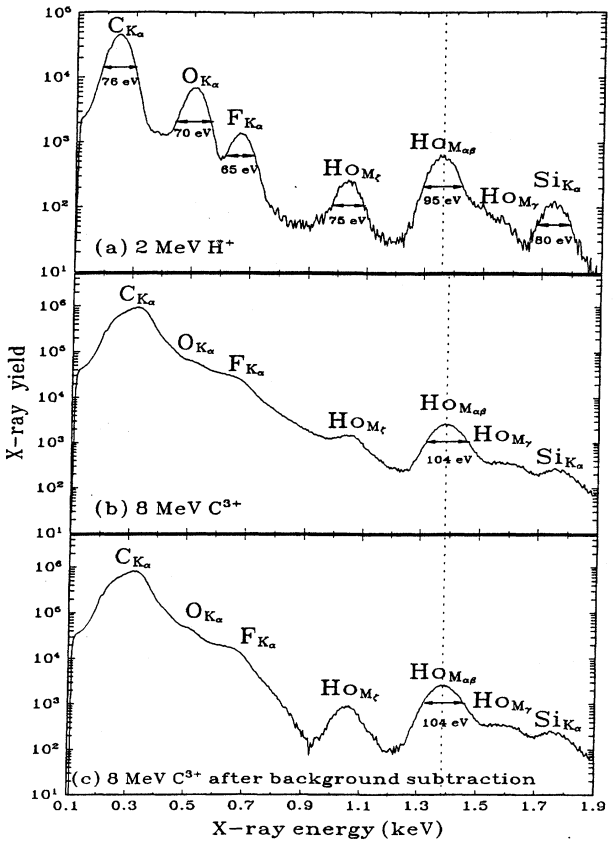

FIG. 2. (a) and (b) are x-ray spectra of HoF_3 produced by 2-MeV H^+ and 8-MeV C^{3+} bombardment, respectively, (c) is a spectrum of (b) after subtraction of the bremsstrahlung background.

target back angle RBS and the gold scattering 90° RBS were measured once for each carbon energy to obtain good counting statistics. Then, for the high-energy ^{12}C data, this ratio could be used to renormalize the back angle scattering where the statistics are poor. This normalization procedure worked very well for all of the data in this article.

IV. DATA ACQUISITION AND REDUCTION

Figure 2(a) shows the pulse height spectrum that was measured for 2-MeV protons on a 0.46-μg/cm^2 HoF_3 target. The HoF_3 was evaporated onto a 5-μg/cm^2 carbon foil to produce these targets. The $_6$C-$K\alpha$ and $_8$O-$K\alpha$ x-ray peaks are from the oxidized carbon foil and the $_9$F-$K\alpha$ x ray is from the HoF_3. The $_{14}$Si-$K\alpha$ (1.74 keV) peak results from the Si (Li) x-ray detector being fluoresced by either backscattered protons that managed to evade the deflection magnet in front of the x-ray detector (see Fig. 1) or photons greater in energy than the Si K-shell binding energy (1.84 keV). It should also be noted that the pulse height spectrum is free from the $_{11}$Na-$K\alpha$ x-ray peak at 1.04 keV. Since a soap solution is used as a surfactant for floating the carbon foils off the glass slides, sodium gets deposited on the foil and is very difficult to remove. The IBMAL laboratory at UNT has developed the techniques to produce contaminant-free targets [28,38,61,62]. The three $_{67}$Ho M-shell x rays of interest are the $M\zeta$, $M_{\alpha\beta}$, and $M\gamma$ peaks. The FWHM resolution of the $_{67}$Ho $M\alpha,\beta$ peak [see Fig. 2(a)] was around 95 eV. This resolution along with the x-ray fitting routines (GUPIX) [68] allowed us to measure the individual cross sections (see Table I) for the $_{67}$Ho M-shell x-ray peaks, $M\zeta$, $M\alpha,\beta$, and $M\gamma$. The situation is more complex when the projectile is changed from $^1_1$H to $^{12}_6$C as is seen in Figs. 2(b) and 2(c). There are several effects that tend to mask the peaks of interest. The most pronounced of these is the carbon ion induced bremsstrahlung from the target backing and projectile. This background is seen for all of the energies of interest in the present work.

Figure 3 shows the measured bremsstrahlung background for a thin carbon foil as a function of incident carbon energy. From this figure, it can be seen that the bremsstrahlung extends out to about 1.3 keV for 2-MeV carbon ions and to almost 2.7 keV for 12-MeV carbon ions. There is obviously some bremsstrahlung produced by the HoF_3 component of the target for Fig. 2 but for the charge-state dependence studies, with a 0.34-μg/cm^2 Ho target, this background bremsstrahlung was certainly minimized.

The other effects that tend to complicate the $_{67}$Ho pulse height spectrum in Fig. 2(b) are the long x-ray tails from the carbon backing and the broadening and shifting of the peaks to higher energies, probably due to some multiple ionization. In order to account for the tailing and bremsstrahlung effects, the appropriate carbon foil spectrum in Fig. 3 was subtracted from the pulse height spectrum for carbon and HoF_3 in Fig. 2(b) to give the result shown in Fig. 2(c). The resultant pulse height spectrum shows a pronounced $M\zeta$ peak and, with the GUPIX x-ray stripping program, $M\alpha,\beta$ and $M\gamma$ could be extracted.

As can be seen from Fig. 2 the $M\alpha,\beta$ peak went from a FWHM of 95 eV for incident protons to 104 eV for 8-MeV carbon ions. It is also observed that the $M\alpha,\beta$ peak is shifted $\sim$30 eV for carbon bombardment compared to proton bombardment. Both of these phenomena tend to indicate there is some multiple ionization taking place. The main question is whether this degree of multiple ionization changes the effective fluorescence yield, which would in turn give a different value for the inner-shell ionization cross section, σ_I, since $\sigma_I = \sigma_X/\omega$, where σ_X is the x-ray production cross section and ω is the x-ray fluorescence yield. There appears to be no exhaustive set of data in the literature to make the case either way [69,70]. Multiple ionization as well as x-ray fluorescence yields vary with the type of primary ion and depend on its charge state and energy. Tawara *et al.* [71] showed that the K-shell fluorescence yields were fairly constant for a ^{28}Si solid target but did show variation for SiH_4 gas targets for incident $_9F^{q+}$ ions. A host of other studies have been made [72–74] but the most convincing set of experimental data for the current case was presented by Tunnell, Can, and Bhalla [75]. They showed the energy dependence of the fluorescence yield for a solid Ti target for incident ions $_1$H through $_{17}$Cl with energies 0.5 through 4.5 MeV/u. It was observed that for incident ^{12}C ions, ω varied from 0.225 to 0.243. This is an 8% variation and hence not a serious problem in comparison to other uncertainties such as the efficiency of the detector. But, it is obvious that further study is

TABLE I. M-shell x-ray production cross sections (in kilobarns) of $_{67}$Ho by $^{12}_{6}C^{q+}$ ions with energies, E_1, from 2 to 12 MeV, in charge state $q+$. $\sigma_{M(\zeta)}$, $\sigma_{M(\alpha,\beta)}$, and $\sigma_{M(\gamma)}$ are experimental x-ray production cross sections of $M\zeta$, $M\alpha,\beta$, and $M\gamma$, respectively, which were extracted from x-ray spectrum after GUPIX computer program [68] curve fitting, σ_{MX} is the measured total M-shell x-ray production cross section and $\sigma_{MX}^{\mathrm{ECPSSR}}$ and $\sigma_{MX}^{\mathrm{FB}}$ the theoretical calculation of M-shell x-ray production cross sections for the ECPSSR theory and the first Born approximation, respectively. The inner-shell ionization cross section of the M-shell, σ_{MI}, shown in the last column is calculated by $\sigma_{MI}=\sigma_{MX}/\omega_{MX}$, with $\omega_{MX}=0.011$ [76] as an effective M-shell x-ray fluorescence yield in $_{67}$Ho.

E_1 (MeV)	$q(+)$	$\sigma_{M(\zeta)}$ (kb)	$\sigma_{M(\alpha,\beta)}$ (kb)	$\sigma_{M(\gamma)}$ (kb)	σ_{MX} (kb)	$\sigma_{MX}/\sigma_{MX}^{\mathrm{FB}}$	$\sigma_{MX}/\sigma_{MX}^{\mathrm{ECPSSR}}$	σ_{MI} (kb)
2	2	0.43 ± 0.07	2.55 ± 0.37	0.12 ± 0.03	3.10 ± 0.38	0.29	4.07	282
2	3	0.46 ± 0.08	2.62 ± 0.38	0.12 ± 0.04	3.20 ± 0.39	0.28	4.11	291
2	4	0.57 ± 0.09	2.68 ± 0.37	0.11 ± 0.04	3.36 ± 0.38	0.28	4.24	305
4	2	1.55 ± 0.20	9.03 ± 1.04	0.44 ± 0.08	11.0 ± 1.1	0.29	1.41	1000
4	3	1.84 ± 0.28	9.21 ± 1.19	0.59 ± 0.12	11.6 ± 1.2	0.29	1.44	1055
4	4	1.89 ±0.34	9.26 ±1.20	0.60 ±0.15	11.7 ±1.3	0.27	1.41	1064
4	5	3.37 ±0.49	14.3 ±1.59	0.86 ±0.17	18.6 ± 1.7	0.076	0.40	1691
4	6	5.53 ± 1.29	22.5 ± 4.23	1.33 ± 0.49	29.4 ± 4.4	0.066	0.35	2673
6	3	3.55 ± 0.54	15.9 ± 1.97	1.59 ± 0.30	21.0 ± 2.1	0.32	1.00	1909
6	4	3.94 ± 0.51	16.1 ± 2.08	1.62 ± 0.32	21.7 ± 2.2	0.31	1.00	1973
6	5	5.96 ± 0.81	24.3 ± 2.68	2.88 ± 0.37	32.6 ± 2.8	0.12	0.47	2964
6	6	8.34 ± 1.13	33.3 ± 3.57	3.27 ± 0.69	45.0 ± 3.8	0.097	0.38	4091
8	3	6.68 ± 0.83	25.8 ± 3.41	2.87 ± 0.47	35.4 ± 3.5	0.43	1.06	3218
8	4	6.81 ± 0.95	26.8 ± 3.65	3.02 ± 0.67	36.6 ± 3.8	0.43	1.07	3327
8	5	8.78 ± 1.59	35.1 ± 5.11	3.69 ± 0.82	47.6 ± 5.4	0.18	0.56	4327
8	6	11.4 ± 1.59	42.5 ± 5.77	4.67 ± 0.92	58.6 ± 6.1	0.13	0.43	5327
10	3	9.43 ± 1.40	30.4 ± 3.95	3.24 ± 0.51	43.1 ± 4.2	0.46	0.96	3918
10	4	10.3 ± 1.52	32.0 ± 4.22	3.50 ± 0.70	45.8 ± 4.5	0.47	0.95	4164
10	5	12.0 ± 1.81	36.4 ± 4.80	4.32 ± 0.84	52.7 ± 5.2	0.20	0.56	4791
10	6	16.0 ± 2.41	45.8 ± 6.22	5.16 ± 1.19	67.0 ± 6.8	0.16	0.47	6091
12	4	10.5 ± 1.91	40.5 ± 5.76	4.25 ± 0.68	55.2 ± 6.1	0.52	0.97	5018
12	5	10.5 ± 3.04	45.5 ± 6.37	4.75 ± 0.73	60.7 ± 7.1	0.23	0.59	5518
12	6	15.8 ± 3.96	51.1 ± 9.57	7.54 ± 1.66	74.5 ± 10.5	0.18	0.51	6773

required to gain deeper insight for the observed variations of fluorescence yields.

In the experiment, when the measured x-ray production cross sections are reduced to inner-shell ionization cross sections, the uncertainty of the fluorescence yields should be taken into account if it is well known. For the M-shell x-ray production, the M-shell fluorescence yields are more complicated than the K- and L-shell fluorescence yields and are still not well measured for each projectile-target pair. Therefore in this paper, single-hole fluorescence yields [76] were used to reduce x-ray production cross sections to ionization cross sections.

The assumption of isotropic x-ray emission may not be true for the present M-shell measurements. The anisotropy of x-ray emission results from the ion-induced inner-shell alignment. Both DI and EC give contributions to the inner-shell alignment. Jitschin [77] has given a comprehensive review of the alignment studies in inner-shell processes. For heavy projectile ions, he pointed out that the alignment effects became very small in the high impact velocity region, $v_1/v_{2S}>0.1$. Until now, no detailed experimental study has been performed for heavy-ion induced M-shell alignment for both DI and EC. In order to prove whether M-shell x rays are emitted isotropically, the angular dependence of M-shell x-ray emission yield should be studied in future experiments. For the results in this paper, M-shell x-ray emission was assumed to be isotropic.

Electron capture contributions to the Ho M-shell x-ray production cross sections were determined using the charge-state dependence of the data for vanishingly thin targets approximating single collision conditions (0.34 μg/cm^2). Electron capture to the S (K, L, and M, etc.) shell of an incident ion can only occur if the ion has a vacancy in that shell. In this case, the M-shell x-ray production cross section due to DI plus EC for the carbon ion with charge state q is given by

$$\sigma_{MX}^{\mathrm{total}\,(C^{q+})}=\sigma_{MX}^{\mathrm{DI}}+\sigma_{MX}^{\mathrm{EC}(C^{q+})}. \tag{2}$$

The direct ionization contributions are assumed to be the same for carbon ions with different charge states, which means the interactions between the projectile electrons and the target electrons are assumed to be small. The M-shell x-ray production cross section due to electron capture to double K-shell vacancies in the carbon ion is then given by

$$\sigma_{MX}^{\mathrm{EC}(K\ \mathrm{shell})}=\sigma_{MX}^{\mathrm{EC}(K,L,M\mathrm{shells})+\mathrm{DI}}-\sigma_{MX}^{\mathrm{EC}(L,M\ \mathrm{shells})+\mathrm{DI}}, \tag{3}$$

which also implies the L, M, ... shell EC is the same for the ion with and without a K-shell vacancy. The M-shell x-ray production cross section due to electron capture to one K-shell vacancy is then given by

$$\sigma_{MX}^{\mathrm{EC}[(1/2)K\mathrm{shell}]}=\sigma_{MX}^{\mathrm{EC}[(1/2)K,L,M\ \mathrm{shells}]+\mathrm{DI}}-\sigma_{MX}^{\mathrm{EC}(L,M\ \mathrm{shells})+\mathrm{DI}}, \tag{4}$$

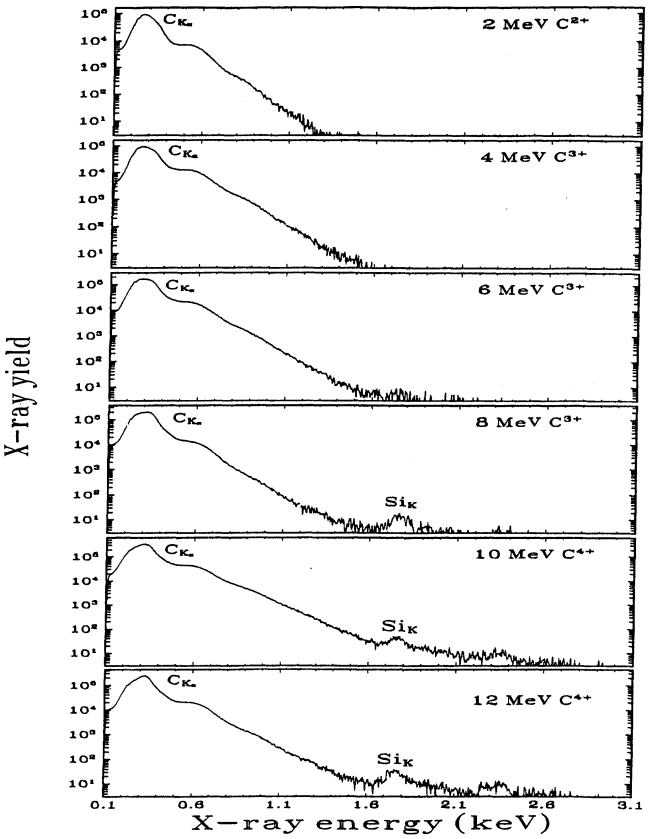

FIG. 3. The background bremsstrahlung spectra from carbon foils by 2–12-MeV carbon ions in different charge states.

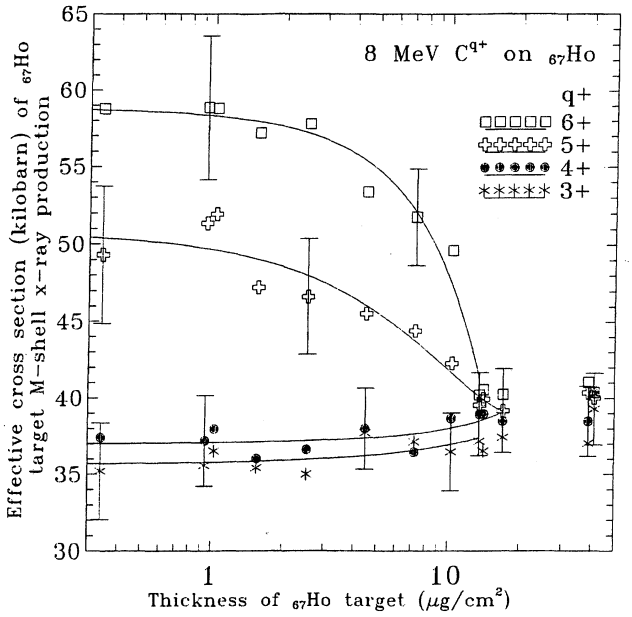

FIG. 4. The "effective" cross section of $_{67}$Ho target M-shell x-ray production by 8-MeV carbon ions for various charge states as a function of target thicknesses. The solid curves are polynomial fits to each data trend.

where $\frac{1}{2}K$ and K represent a half vacant and completely vacant K shell for the incident carbon ion, respectively. This equation also assumes the DI is the same and independent of the number of electrons on the ions.

The effect of the electron carried by the carbon ion incident on the target electron corresponds to an increase in the ionization probability and may be considered to be an electron-correlation process. Usually, the incident electrons play a passive role in screening the projectile nuclear charge and, thus, decrease the ionization probability. However, an incident electron may also participate actively in the collision by ejecting a target electron in a binary electron-electron collision [78–80]. The inner-shell ionization probability due to direct Coulomb ionization for different charge state ions with the same atomic mass may be different because of electron correlation. However, the contribution from the interaction between electrons is not comparable to that between projectile nucleus and target electron. Therefore, the electron-correlation effect is neglected in this study.

V. RESULTS AND DISCUSSION

When a highly charged particle, such as a fully stripped carbon ion, enters a thick target it will lose or gain electrons until the rates are equal and the ions will move towards an equilibrium charge state [81]. For the electron capture measurements, it is important that the incident ion be essentially in the single collision realm. This phenomenon can be studied by measuring the effective cross section of the Ho target M-shell x-ray production for various charge states as a function of target thicknesses. Figure 4 shows the result for 8-MeV $^{12}C^{q+}$ ($q=3-6$) ions incident on $_{67}$Ho targets of thickness varying from 0.34 to 41 μg/cm^2. It can be seen that at a thickness of approximately 14 μg/cm^2 the "effective" cross section for all incident ions is constant (at about 38 kb). Therefore, for targets thicker than 14 μg/cm^2, all incident 8-MeV $^{12}C^{3+-6+}$ ions reach the equilibrium charge state. The most important region of Fig. 4 is the thin target region that shows the plateau for each charge state. From Fig. 4, it can be seen that below $\sim$2 μg/cm^2, single collision conditions are maintained. To be certain of single collision conditions, all of the electron capture data reported in this paper were for a $_{67}$Ho target of 0.34-μg/cm^2 thickness. This thickness gives an areal density of 1.24×10^{15} atoms/cm^2, which is between 1 and 2 atomic layers.

Table I contains a summary of the present data. It includes the $M\zeta$, $M\alpha,\beta$, and $M\gamma$ x-ray contributions and the total M-shell x-ray production cross sections. The experimental uncertainties were determined from all contributions related to the experiment. For the measured efficiency of the x-ray detector, the error was estimated to be 12–16% after calibration by several methods. The solid angle of the particle detector was measured by an ^{241}Am source with a 1.3% uncertainty. Assuming Rutherford scattering, the error in the backscattering cross section for beam energy fluctuation did not exceed 2% since our studies are considerably below the Coulomb barrier [82,83] at 12 MeV and the screening effect [84] at 2 MeV was estimated to be below 0.5%. The uncertainty in the yield of backscattered particles increased with the projectile energy from 3% to 7% due to counting statis-

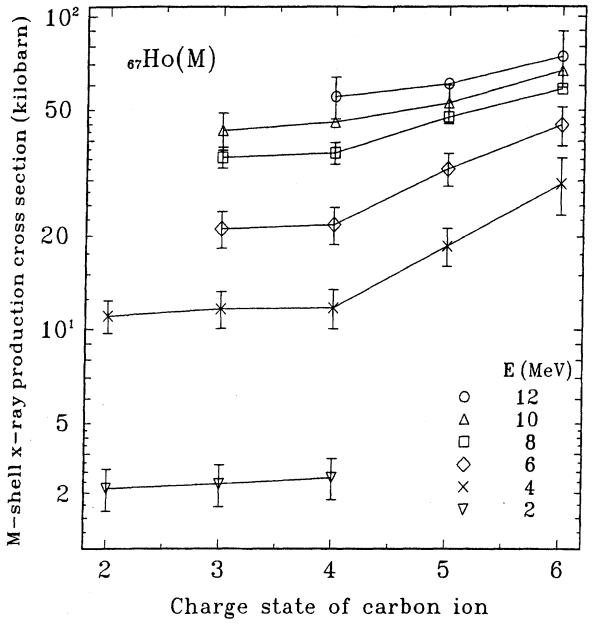

FIG. 5. Charge-state dependence of M-shell x-ray production in a 0.34-μg/cm^2 $_{67}$Ho target by 2–12-MeV carbon ions in charge states from 2+ to 6+.

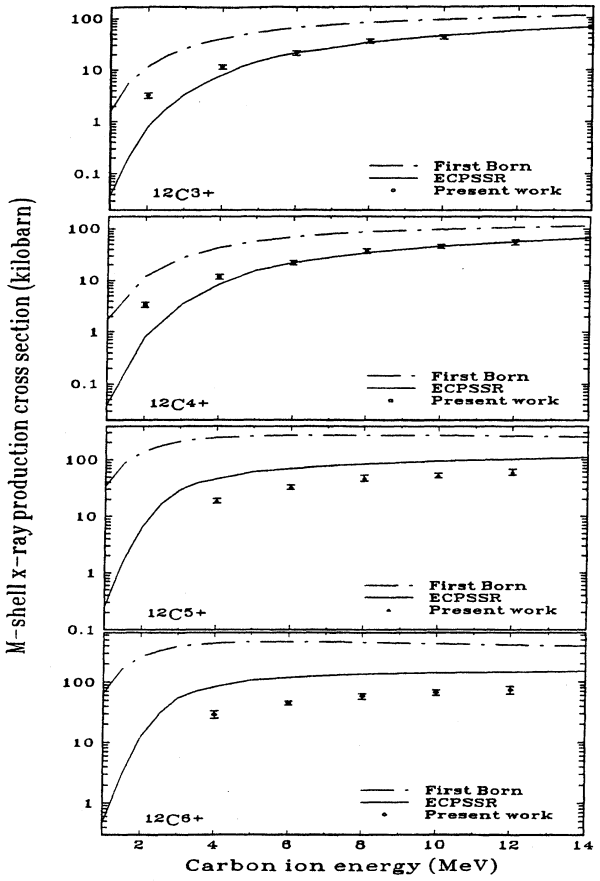

FIG. 6. M-shell x-ray production in $_{67}$Ho by carbon ions in charge state 3+, 4+, 5+, and 6+ with theoretical calculations of the first Born approximation (dashed-dot curve) and the ECPSSR theory (solid curve).

tics. The curve fitting procedure for the x-ray spectra was the major source of uncertainty. To minimize the uncertainties, the following precautions were carried out. The long tail of the carbon K-shell x-ray peak had to be subtracted from the $M\zeta$ peak. Similarly, the $M\gamma$ peak had to be stripped from the pronounced $M\alpha,\beta$ peak. The Si $K\alpha$ peak was also subtracted from $M\gamma$ region. Hence, as shown in Table I, the uncertainties associated with each x-ray peak ranged from 17% to 37%. Also displayed in Table I are the ratios of experimental M-shell x-ray production to the theoretical calculations of the first Born and ECPSSR theories for $^{12}C^{q+}$ ($q=2-6$) and carbon ion energies between 2 and 12 MeV. Figure 5 shows the projectile charge-state dependences of the total M-shell x-ray production cross sections of $_{67}$Ho by 2–12-MeV carbon ions. The cross sections for charge states 2+ to 4+ are almost flat, indicating that the electron capture contribution for carbon ions without a K vacancy ($L,M,\ldots$ shell EC) is small comparing to that for carbon ions with K-shell vacancies. For carbon ions with K-shell vacancies ($q=5+$ and 6+), the cross section increases from as little as 10% (at 12-MeV $q=5+$) to 150% (at 4-MeV $q=6+$) compared to the data for $q=4+$.

Figure 6 shows a plot of the total M-shell x-ray production cross sections as a function of energy for four charge states used in this report. Also shown in the figure are the theoretical predictions of the first Born and ECPSSR theories. It can be seen that the ECPSSR theory fits the $q=3+$ and 4+ data (DI+EC to $L,M,\ldots$ shells) quite well for the carbon energies 6–12 MeV. However, it overpredicts the $q=5+$ and 6+ data (DI+EC to $K,L,M,\ldots$ shells) at all energies by 170–290%. The first Born approximation is seen to overpredict all the experimental data at all energies by a significant amount up to factors of 15. The first Born approximation was originally calculated for high velocity ion-atom collisions. At a velocity ratio range, $0.17\leq v_1/v_{2M}<0.42$, the carbon ion velocity is less than the M-shell electron velocity, it may be reasonable for the first Born theory to give an overestimation of the cross sections. The apparent agreement of the data with the ECPSSR theory for $q=3+$ and $q=4+$ at 6–12 MeV possibly could be fortuitous and due to contributions from carbon electron-target electron interactions that are not as possible for the highly charged ions with fewer electrons or due to the overestimation of the EC to $L,M,\ldots$ shells that makes up for the underestimation of the DI.

Gardner *et al.* [85] suggested consideration of the EC to $L,M,\ldots$ shells for heavy ion collisions and added it to the DI in the theoretical model for the total ionization cross section in order to compare with their experiment. Their combination of data shows that the ECPSSR theory for the sum of DI and EC to $L,M,\ldots$ shells gives excellent agreement to the data. However, Tanis *et al.* [86] mentioned that the EC to $L,M,\ldots$ shells may be very small and can be neglected from their results of Ti K-shell x-ray production cross sections for $_{17}$Cl ions with charge state 7+ (DI+EC to $M,N,\ldots$ shells) and 15+ (DI+EC to $L,M,N,\ldots$ shells). Tanis *et al.* [86] suggested inclusion of the molecular orbital

TABLE II. Contribution of electron capture to M-shell x-ray production cross sections (in kilobarns) in Ho by carbon ions with K-shell vacancies ($q=5+$ and $6+$) at energies $E_1=4-12$ MeV. The experimental M-shell x-ray production cross sections due to electronic capture, σ_{MX}^{EC}, were calculated from the difference of Ho total M-shell x-ray cross sections for carbon ions with and without K-shell vacancies. $\sigma_{MX}^{EC\text{-}ECPSSR}$ and $\sigma_{MX}^{EC\text{-}FB}$ are the theoretical contributions of electron capture to the K-shell from the ECPSSR theory and the first Born approximation, respectively.

E_1 (MeV)	q (+)	$\sigma_{MX}^{EC}(q)=\sigma_{MX}(q)-\sigma_{MX}(4)$ (kb)	$\sigma_{MX}^{EC}(q)/\sigma_{MX}^{EC\text{-}FB}(q)$	$\sigma_{MX}^{EC}(q)/\sigma_{MX}^{EC\text{-}ECPSSR}(q)$
4	5	6.9 ± 2.1	0.030	0.17
4	6	17.7 ± 4.6	0.041	0.22
6	5	10.9 ± 3.6	0.045	0.19
6	6	23.3 ± 4.4	0.053	0.22
8	5	11.0 ± 6.6	0.048	0.18
8	6	22.0 ± 7.2	0.053	0.20
10	5	6.9 ± 6.9	0.032	0.11
10	6	21.2 ± 8.2	0.056	0.19
12	5	5.5 ± 9.36	0.028	0.10
12	6	19.3 ± 12.1	0.055	0.19
E_1 (MeV)	q (+)	$\sigma_{MX}^{EC}(q)=\sigma_{MX}(q)-\sigma_{MX}(3)$ (kb)	$\sigma_{MX}^{EC}(q)/\sigma_{MX}^{EC\text{-}FB}(q)$	$\sigma_{MX}^{EC}(q)/\sigma_{MX}^{EC\text{-}ECPSSR}(q)$
4	5	7.0 ± 2.1	0.030	0.17
4	6	17.8 ± 4.6	0.041	0.23
6	5	11.6 ± 3.5	0.048	0.21
6	6	24.0 ± 4.3	0.055	0.23
8	5	12.2 ± 6.4	0.053	0.20
8	6	23.2 ± 7.0	0.056	0.21
10	5	9.6 ± 6.7	0.044	0.17
10	6	23.9 ± 8.0	0.063	0.22

effect instead of the EC to $L,M,\ldots$ shells for comparison with the data.

As seen in Fig. 6, the ECPSSR theory underestimates the data (DI+EC to $L,M,\ldots$ shells) at 2- and 4-MeV $C^{3+,4+}$. This may be caused by (1) the modification factors for energy loss, Coulomb deflection, and relativistic effects reduce the cross sections too much in this low-energy region, (2) some multiple ionization exists for slow heavy ion bombardment which increases the fluorescence yields [31], (3) projectile electron-target electron interaction increases the x-ray production and is not included in the theory, or (4) quasimolecular orbital channels might give an additional contribution to inner shell ionization although this contribution—judging by Fig. 10 of Ref. [86]—may not be critical in the region of our experiment where $Z_1/Z_2=0.09$ and $0.17\leq v_1/v_{2M}<0.42$.

One might interpret the observed discrepancy at 2 MeV as an overestimation of the binding effect as calculated in the perturbed stationary-state approach of the ECPSSR theory. For L_1 subshell ionization of $_{70}$Yb by $_7$N, where $Z_1/Z_2=0.10$ is comparable to our Z_1/Z_2 value, coupled-channel calculations of Shingal, Malhi, and Gray [87] result in larger cross sections than predicted by the ECPSSR theory. The importance of the L-shell intrashell couplings has been stressed and studied by Sarkadi and Mukoyama [88]; the inclusion of this effect somewhat spoils the ECPSSR agreement with the data and it makes substantial improvement for the L_2 subshell ionization for low-velocity heavy ions [89]. One could argue that the enhancement due to intrashell coupling would be more pronounced for less tightly bound electrons of the M shell.

Just as the total L-shell ionization is essentially not affected by the neglect of intrashell coupling, however, it is not necessary to account for this effect in our analysis of total M-shell ionization. Cross sections for M-shell ionization of Th and U by 2.5–4.5-MeV α particles [92] are overshadowed by contributions from the outermost M subshells, which are well predicted by the ECPSSR theory. In the very similar v_1/v_{2M} range of our experiment, the total M-shell ionization is also dominated by contributions from its outermost subshells: M_4 and M_5 contribute nearly 80% while M_1 is less than 2% of the M-shell ionization cross section. Given that intrashell couplings play almost no role in the outermost L-subshell, i.e., L_3, ionization [88,89], we infer than indeed coupled channel calculations would not yield significantly different results than the ECPSSR theory.

Table II tabulates contributions of electron capture to $_{67}$Ho M-shell x-ray production cross sections and ratios to the corresponding ECPSSR and first Born theories. In Table II, the $_{67}$Ho M-shell x-ray production cross sections with all the $q=4+$ data for 4 to 12 MeV and with the $q=3+$ data for 4 to 10 MeV used for subtraction. No data for $q=3+$ at

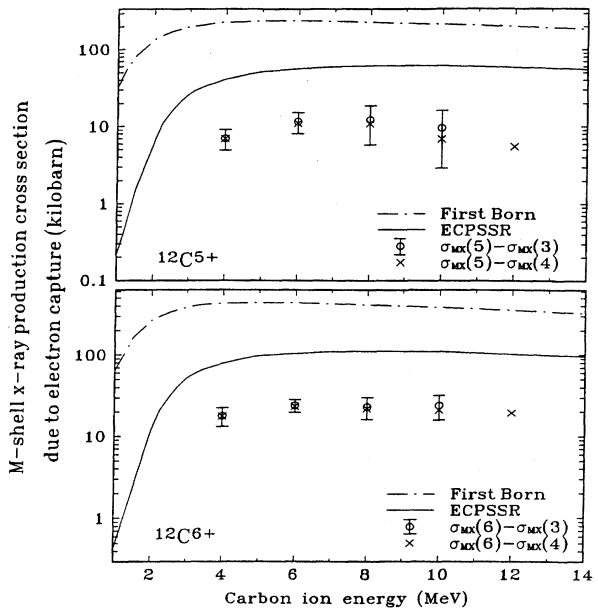

FIG. 7. M-shell x-ray production in $_{67}$Ho due to electron capture to the ion as a function of incident carbon ion energy from 4 to 12 MeV for H-like and fully stripped carbon ions. Both the first Born approximation (dash-dot curve) and the ECPSSR theory (solid curve) for the electron capture overestimate the data.

12 MeV was gathered because usable quantities of this ion could not be produced. These electron capture contributions were obtained by subtracting the M-shell x-ray production cross sections for $q=3+$ or $4+$ from those of $q=5+$ and $6+$ as mentioned earlier using Eqs. (3) and (4). This difference should give the contribution of electron capture into the hydrogenlike ($q=5+$) or bare ($q=6+$) carbon ions. The results with $q=4+$ subtracted from the data may be lower than the results with $q=3+$ subtracted from the data (see 10-MeV data of Table II and Fig. 7) because the experimental cross sections of $q=4+$ might be slightly higher than that of $q=3+$. This occurs when He-like carbon ions are produced in the accelerator terminal gas stripper in a metastable state with one electron in the $1s$ state and another one in the $2s$ state. This $1s2s$ metastable state can also be formed when passing through the postaccelerator stripper [90,91]. Depending on the stripper thickness, the percentage of ions left in a metastable state can be 10–20% [23]. If the metastable ion's lifetime is longer than its transient time to bombard the target, this metastable ion with charge state $q+=Z_2-2$ may allow some electron capture contributions similar to that of the $q+=Z_2-1$ ion during collision. As a result, the metastable state condition of a heliumlike carbon ion ($q=4+$) may contribute a small enhancement to the x-ray production cross section due to electron capture. Figure 7 shows the extracted cross sections of EC to the K shell for carbon ions in charge states $q=5+$ and $6+$. Also shown in Fig. 7 are the theoretical predictions of the first Born and ECPSSR theories for EC. The ECPSSR theory is seen to overpredict the measurements by a factor of 4–10 while the first Born (OBKN) calculations are at least a factor of 16 higher than the experimental results.

VI. CONCLUSIONS

The "effective" cross sections of $_{67}$Ho target M-shell x-ray production for 2–12-MeV $_6$C ions in various charge states were measured as a function of target thicknesses (see Fig. 4). It is clear from these studies that single collision conditions exist for target thicknesses less than ~ 2 μg/cm^2. To be certain of single collision conditions, all of the cross-section measurements for charge-state dependence of the M-shell x-ray production reported in this paper were done with a $_{67}$Ho target that was 0.34 μg/cm^2 thick, which is approximately 1–2 atomic layers. The data were found to be reproducible for these thin targets. The charge-state dependence of M-shell x-ray production cross sections of $_{67}$Ho were then measured in this single collision regime for $^{12}C^{q+}$ ($q=2+$ to $6+$) ions from 2 to 12 MeV (see Fig. 5). It was not possible to reach charge states $5+$ and $6+$ for the 2-MeV data since the stripping cross sections are simply too low. The cross sections for $q=2+$ to $4+$ (no K vacancy) are seen to be significantly lower than those for $q=5+$ and $6+$, indicating in the latter cases contributions to the inner-shell ionization from electron capture into the K-shell of ^{12}C.

The numerical value of the measured electron capture cross section was determined by subtracting the $q=3+$ or $4+$ data from the $q=5+$ and $6+$ data for vanishingly thin targets. The electron capture cross sections were then compared to the theoretical calculations of the first Born and ECPSSR theories (see Fig. 7). The ECPSSR theory seems to be about a factor of 4 higher than the experimental results while the first Born theory gave results that were about a factor of 16 higher than the measured results. For the total M-shell x-ray production cross sections, the ECPSSR theory gives a good fit to the experimental data for average charge states near the equilibrium value (see Fig. 6) at 6 to 12 MeV. It still underestimates the data at 2 and 4 MeV. In the low-energy region, the molecular orbital (MO) effects and multiple ionization may become important and should contribute to higher ionization cross section. The first Born theory, however, overpredicts the experimental data by about a factor of 2–15 over most of the energy range.

In this paper, it has been shown that electron capture to carbon ions with K vacancies is a major contributor (10–60%) to the M-shell ionization in addition to direct Coulomb ionization. The theories give a good fit to the data for the sum of DI and EC to $L,M,\ldots$ shells, but do not give an accurate prediction for EC for the region $Z_1/Z_2=0.09$ and $0.17\leq v_1/v_{2M}<0.42$. Inner-shell ionization is a very complicated process that is related to several mechanisms and varies for different collision systems. Further study of M-shell ionization by heavy ions is required for those unknown terms that include the MO effects at low energy, the electron correlation contribution to both DI and EC, the multiple ionization, and all the parameters related to fluorescence yields, and the M-shell x-ray isotropy.

ACKNOWLEDGMENTS

This work was supported in part by the Office of Naval Research, National Science Foundation, and the Robert A. Welch Foundation.

[1] H. D. Betz, Rev. Mod. Phys. **44**, 465 (1972).
[2] N. Bohr, K. Dansk. Vidensk. Selsk. Mat. Fys. Medd. **18**, 8 (1948).
[3] S. K. Allison and S. D. Warshaw, Rev. Mod. Phys. **25**, 779 (1953); S. K. Allison, *ibid.* **30**, 1137 (1958).
[4] J. R. Macdonald, L. Winters, M. D. Brown, T. Chiao, and L. D. Ellsworth, Phys. Rev. Lett. **29**, 1291 (1972).
[5] J. R. Macdonald, L. M. Winters, M. D. Brown, L. D. Ellsworth, T. Chaio, and E. W. Pettus, Phys. Rev. Lett. **30**, 251 (1973).
[6] J. R. Mowat, D. J. Pegg, R. S. Peterson, P. M. Griffin, and I. A. Sellin, Phys. Rev. Lett. **29**, 1577 (1972); S. Datz, R. S. Thoe, and I. A. Sellin, *ibid.* **33**, 733 (1973).
[7] W. Brandt, R. Laubert, M. Maurino, and A. Schwarzschild, Phys. Rev. Lett. **30**, 358 (1973).
[8] A. M. Halpern and J. Law, Phys. Rev. Lett. **31**, 4 (1973).
[9] J. R. Macdonald, C. L. Cocke, and W. W. Edison, Phys. Rev. Lett. **32**, 648 (1974); S. J Czuchlewski, J. R. Macdonald, and L. D. Ellsworth, Phys. Rev. A **11**, 1108 (1975).
[10] F. Hopkins, R. L. Kauffman, C. W. Woods, and P. Richard, Phys. Rev. A **9**, 2413 (1974); F. Hopkins, Phys. Rev. Lett. **35**, 270 (1975).
[11] J. R. Macdonald, M. D. Brown, S. J. Czuchlewski, L. M. Winters, R. Laubert, I. A. Sellin, and J. R. Mowat, Phys. Rev. A **14**, 1997 (1976).
[12] T. J. Gray, P. Richard, R. L. Kauffman, T. C. Holloway, R. K. Gardner, G. M. Light, and J. Guertin, Phys. Rev. A **13**, 1344 (1976).
[13] T. J. Gray, P. Richard, R. K. Gardner, K. A. Jamison, and J. M. Hall, Phys. Rev. A **14**, 1333 (1976).
[14] R. K. Gardner, T. J. Gray, P. Richard, C. Schmiedekamp, K. A. Jamison, and J. M. Hall, Phys. Rev. A **15**, 2202 (1977).
[15] J. A Guffey, L. D. Ellsworth, and J. R. Macdonald, Phys. Rev. A **15**, 1863 (1977).
[16] U. Schiebel, T. J. Gray, R. K. Gardner, and P. Richard, J. Phys. B **10**, 2189 (1977).
[17] T. J. Gray, C. L. Cocke, and R. K. Gardner, Phys. Rev. A **16**, 1907 (1977).
[18] B. Doyle, U. Schiebel, J. R. Macdonald, and L. D. Ellsworth, Phys. Rev. A **17**, 523 (1978).
[19] H. Tawara, P. Richard, T. J. Gray, J. Newcomb, K. A. Jamison, C. Schmiedekamp, and J. M. Hall, Phys. Rev. A **18**, 1373 (1978).
[20] C. Schmiedekamp, T. J. Gray, B. L. Doyle, and U. Schiebel, Phys. Rev. A **19**, 2167 (1979).
[21] T. J. Gray, P. Richard, G. Gealy, and J. Newcomb, Phys. Rev. A **19**, 1424 (1979).
[22] J. R Oppenheimer, Phys. Rev. **31**, 349 (1928); H. C. Brinkman and H. A. Kramers, Proc. Acad. Sci. (Amsterdam) **33**, 973 (1930).
[23] F. D. McDaniel, J. L. Duggan, G. Basbas, P. D. Miller, and G. Lapicki, Phys. Rev. A **16**, 1375 (1977).
[24] G. Lapicki and W. Losonsky, Phys. Rev. A **15**, 896 (1977).
[25] F. D. McDaniel, A. Toten, R. S. Peterson, J. L. Duggan, S. R. Wilson, J. D. Gressett, P. D. Miller, and G. Lapicki, Phys. Rev. A **19**, 1517 (1979).
[26] R. Mehta, J. L. Duggan, F. D. McDaniel, M. C. Andrews, R. M. Wheeler, R. P. Chaturvedi, P. D. Miller, and G. Lapicki, IEEE Trans. Nucl Sci. **NS-28**, 1122 (1981).
[27] R. Mehta, J. L. Duggan, F. D. McDaniel, M. C. Andrews, G. Lapicki, P. D. Miller, L. A. Rayburn, and A. R. Zander, IEEE Trans. Nucl. Sci. **NS-30**, 906 (1983).
[28] R. Mehta, J. L. Duggan, F. D. McDaniel, M. C. Andrews, G. Lapicki, P. D. Miller, L. A. Rayburn, and A. R. Zander, Phys. Rev. A **28**, 2722 (1983).
[29] M. C. Andrews, F. D. McDaniel, J. L. Duggan, P. D. Miller, P. L. Pepmiller, H. F. Krause, T. M. Rosseel, L. A. Rayburn, R. Mehta, and G. Lapicki, Nucl. Instrum. Methods Phys. Res. Sect. B **10/11**, 186 (1985).
[30] M. C. Andrews, F. D. McDaniel, J. L. Duggan, R. Mehta, G. Lapicki, P. D. Miller, P. L. Pepmiller, H. F. Krause, T. M. Rosseel, and L. A. Rayburn, Nucl. Instrum. Methods Phys. Res. Sect. B **10/11**, 181 (1985).
[31] G. Lapicki, R. Mehta, J. L. Duggan, P. M. Kocur, J. L. Price, and F. D. McDaniel, Phys. Rev. A **34**, 3813 (1986).
[32] J. L. Price, J. L. Duggan, F. D. McDaniel, G. Lapicki, and R. Mehta, Phys. Rev. A **34**, 2830 (1986).
[33] M. C. Andrews, F. D. McDaniel, J. L. Duggan, P. D. Miller, P. L. Pepmiller, H. F. Krause, T. M. Rosseel, L. A. Rayburn, R. Mehta, and G. Lapicki, Phys. Rev. A **36**, 3699 (1987).
[34] J. L. Price, J. L. Duggan, F. D. McDaniel, G. Lapicki, and R. Mehta, Phys. Rev. A **37**, 365 (1988).
[35] F. D. McDaniel, J. L. Duggan, G. Lapicki, and P. D. Miller, Nucl. Instrum. Methods Phys. Res. Sect. B **42**, 485 (1989).
[36] Y. C. Yu, M. R. McNeir, D. L. Weathers, J. L. Duggan, F. D. McDaniel, and G. Lapicki, Phys. Rev. A **44**, 5702 (1991).
[37] Y. C. Yu, M. R. McNeir, D. L. Weathers, J. L. Duggan, F. D. McDaniel, D. K. Marble, Z. Y. Zhao, and G. Lapicki, Phys. Rev. A **44**, 7252 (1991).
[38] F. D. McDaniel, D. K. Marble, J. L. Duggan, M. R. McNeir, Y. C. Yu, Z. Y. Zhao, D. L. Weathers, R. M. Wheeler, R. P. Chaturvedi, and G. Lapicki, Nucl. Instrum. Methods Phys. Res. Sect. B **53**, 531 (1991).
[39] Y. C. Yu, M. R. McNeir, D. L. Weathers, D. K. Marble, J. L. Duggan, F. D. McDaniel, and G. Lapicki, Nucl. Instrum. Methods Phys. Res. Sect. B **56/57**, 1188 (1991).
[40] M. C. McNeir, Y. C. Yu, D. L. Weathers, D. K. Marble, J. L. Duggan, F. D. McDaniel, and G. Lapicki, Nucl. Instrum. Methods Phys. Res. Sect. B **56/57**, 26 (1991).
[41] D. K. Marble, F. D. McDaniel, M. C. McNeir, Y. C. Yu, Z. Y. Zhao, D. K. Wilson, D. L. Weathers, J. L. Duggan, R. M. Wheeler, R. P. Chaturvedi, G. Lapicki, and V. Zoran, Nucl. Instrum. Methods Phys. Res. Sect. B **56/57**, 33 (1991).
[42] R. Mehta, J. L. Duggan, F. D. McDaniel, M. C. McNeir, Y. C. Yu, D. K. Marble, and G. Lapicki, Nucl. Instrum. Methods Phys. Res. Sect. B **79**, 175 (1993).
[43] H. L. Sun, J. F. Kirchhoff, A. R. Azordegan, J. L. Duggan, F. D. McDaniel, R. M. Wheeler, R. P. Chaturvedi, and G. Lapicki, Nucl. Instrum. Methods Phys. Res. Sect. B **79**, 194 (1993).
[44] H. L. Sun, J. F. Kirchhoff, A. R. Azordegan, J. L. Duggan, F. D. McDaniel, R. M. Wheeler, R. P. Chaturvedi, and G. Lapicki, Nucl. Instrum. Methods Phys. Res. Sect. B **79**, 186 (1993).
[45] D. E. Johnson, G. Basbas, and F. D. McDaniel, At. Data Tables **24**, 1 (1979).
[46] V. S. Nikolaev, Zh. Eksp. Teor. Fiz. **51**, 1263 (1966) [Sov. Phys. JETP **24**, 847 (1967)].
[47] W. Brandt and G. Lapicki, Phys. Rev. A **23**, 1717 (1981).
[48] G. Basbas, W. Brandt, and R. Laubert, Phys. Rev. A **7**, 983 (1973); **17**, 1655 (1978).

[49] G. Barbas, W. Brandt, and R. H. Ritchie, Phys. Rev. A **7**, 1971 (1973).
[50] G. Lapicki and F. D. McDaniel, Phys. Rev. A **22**, 1896 (1980); **23**, 975(E) (1981).
[51] E. Merzbacher and H. Lewis, *Handbuch der Physik*, edited by S. Flugge (Springer, Berlin, 1958), Vol. 34, p. 166.
[52] U. Fano and W. Licten, Phys. Rev. Lett. **14**, 627 (1965).
[53] W. Lichten, Phys. Rev. **164**, 131 (1967).
[54] M. Barat and W. Lichten, Phys. Rev. A **6**, 211 (1972).
[55] W. Meyerhof, Phys. Rev. A **18**, 414 (1978); **20**, 2235 (1979).
[56] R. Anholt, Rev. Mod. Phys. **57**, 995 (1985).
[57] G. Lapicki and W. Lichten, Phys. Rev. A **31**, 1354 (1985).
[58] H. A. Bethe, Ann. Phys. **5**, 325 (1930).
[59] G. Lapicki, Phys. Chem. Ref. Data **18**, 111 (1989).
[60] M. C. McNeir, Y. C. Yu, D. L. Weathers, D. K. Marble, J. L. Duggan, F. D. McDaniel, and G. Lapicki, Nucl. Instrum. Methods Phys. Res. Sect. B **56/57**, 26 (1991); M. C. McNeir, Y. C. Yu, D. L. Weathers, J. L. Duggan, F. D. McDaniel, and G. Lapicki, Phys. Rev. A **44**, 4372 (1991).
[61] D. K. Marble, Ph.D. thesis, University of North Texas, 1991.
[62] D. L. Weathers, J. L. Duggan, R. B. Escue, F. D. McDaniel, Nucl. Instrum. Methods Phys. Res. Sect. A **303**, 69 (1991).
[63] R. G. Musket, Nucl. Instrum. Methods Phys. Res. Sect. B **15**, 735 (1986).
[64] J. L. Campbell and L. A. McNelles, Nucl. Instrum. Methods **125**, 205 (1975).
[65] W. N. Lennard and D. Phillips, Nucl. Instrum. Methods **166**, 521 (1979).
[66] D. L. Weathers, J. L. Duggan, M. C. McNeir, Y. C. Yu, F. D. McDaniel, C. A. Quarles, H. Lehtihet, and D. Kahler, Nucl. Instrum. Methods Phys. Res. Sect. B **56/57**, 964 (1991).
[67] Wm. J. Veigele, At. Data Tables **5**, 51 (1973).
[68] J. A. Maxwell, J. L. Campbell, and W. J. Teesdale, Nucl. Instrum. Methods Phys. Res. Sect. B **43**, 218 (1989).
[69] D. Burch, N. Stolterfoht, D. Schneider, H. Wieman, and J. S. Risley, Phys. Rev. Lett. **32**, 1151 (1974).
[70] L. Winter, J. R. Macdonald, M. D. Brown, T. Chiao, L. D. Ellsworth, and E. W. Pettus, Phys. Rev. A **8**, 1835 (1973).
[71] H. Tawara, P. Richard, T. J. Gray, J. R. Macdonald, and R. Dillingham, Phys. Rev. A **19**, 2131 (1979).
[72] J. R. Mowat, D. J. Pegg, R. S. Peterson, P. M. Griffin, and I. A. Sellin, Phys. Rev. Lett. **29**, 1577 (1972).
[73] J. R. Mowat, I. A. Sellin, P. M. Griffin, D. J. Pegg, and R. S. Peterson, Phys. Rev. A **9**, 644 (1974).
[74] C. D. Lin and P. Richard, in *Advances in Atomic and Molecular Physics*, edited by S. D. Bates and B. Bederson (Academic, New York, 1981), pp. 275–353.
[75] T. W. Tunnell, C. Can, and C. P. Bhalla, IEEE Trans. Nucl. Sci. **NS-26**, 1124 (1979).
[76] E. J. Muggier, Phys. Rev. A **5**, 1043 (1972).
[77] W. Jitschin, in *X-ray and Atomic Inner-shell Physics—1982*, edited by B. Crasemann (American Institute of Physics, New York, 1982), pp. 74–84.
[78] D. R. Bates and G. W. Griffing, Proc. Phys. Soc. London A **66**, 961 (1953).
[79] J. S. Briggs and K. Taulbjerg, in *Structure and Collisions of Ions and Atoms*, edited by I. A. Sellin (Springer-Verlag, Heidelberg, 1978), p. 105.
[80] J. H. McGuire, N. Stolterfoht, and P. R. Simony, Phys. Rev. A **24**, 97 (1981).
[81] T. J. Gray, in *Methods of Experimental Physics*, edited by P. Richard (Academic, New York, 1980), Vol. 17, p. 193.
[82] M. Bozoian, K. M. Hubbard, and M. Nastasi, Nucl. Instrum. Methods Phys. Res. Sect. B **51**, 311 (1990).
[83] M. Bozoian, Nucl. Instrum. Methods Phys. Res. Sect. B **56/57**, 740 (1991).
[84] H. H. Andersen, F. Besenbacher, P. Loftager, and W. Möller, Phys. Rev. A **21**, 1891 (1980).
[85] R. K. Gardner, T. J. Gray, P. Richard, C. Schmiedekamp, K. A. Jamison, and J. M. Hall, Phys. Rev. A **19**, 1896 (1979).
[86] J. A. Tanis, S. M. Shafroth, W. W. Jacobs, T. McAbee, and G. Lapicki, Phys. Rev. A **31**, 750 (1985).
[87] R. Shingal, N. B. Malhi, and T. J. Gray, J. Phys. B **25**, 2055 (1992).
[88] L. Sarkadi and T. Mukoyama, J. Phys. B **13**, 2255 (1980); **23**, 3849 (1990); Nucl. Instrum. Methods Phys. Res. Sect. B **61**, 167 (1991).
[89] M. Sarkar, D. Bhattacharya, M. B. Chatterjee, P. Sen, G. Kuri, D. P. Mahparta, and G. Lapicki (to be published).
[90] I. A. Sellin, Adv. At. Mol. Phys. **12**, 215 (1977).
[91] C. D. Lin, W. R. Johnson, and A. Dalgarno, Phys. Rev. A **15**, 154 (1977).
[92] X. Cai, Z. Y. Liu, X. M. Chen, S. X. Ma, Z. C. Chen, Q. Xu, H. P. Liu, and X. W. Ma, Phys. Scr. **47**, 751 (1993).